Drug Delivery Hot Paper

Deutsche Ausgabe: DOI: 10.1002/ange.201604858
Internationale Ausgabe: DOI: 10.1002/anie.201604858

Multistimuli-Responsive Bilirubin Nanoparticles for Anticancer Therapy

*Yonghyun Lee, Soyoung Lee, Dong Yun Lee, Byeongjun Yu, Wenjun Miao, and Sangyong Jon**

Abstract: *Although stimuli-responsive materials hold potential for use as drug-delivery carriers for treating cancers, their clinical translation has been limited. Ideally, materials used for the purpose should be biocompatible and nontoxic, provide "on-demand" drug release in response to internal or external stimuli, allow large-scale manufacturing, and exhibit intrinsic anticancer efficacy. We present multistimuli-responsive nanoparticles formed from bilirubin, a potent endogenous antioxidant that possesses intrinsic anticancer and anti-inflammatory activity. Exposure of the bilirubin nanoparticles (BRNPs) to either reactive oxygen species (ROS) or external laser light causes rapid disruption of the BRNP nanostructure as a result of a switch in bilirubin solubility, thereby releasing encapsulated drugs. In a xenograft tumor model, BRNPs loaded with the anticancer drug doxorubicin (DOX@BRNPs), when combined with laser irradiation of 650 nm, significantly inhibited tumor growth. This study suggests that BRNPs may be used as a drug-delivery carrier as well as a companion medicine for effectively treating cancers.*

Since the first emergence and successful application of thermosensitive liposomes in the 1970s,[1] stimulus-responsive materials have attracted considerable attention[2] as drug-delivery carriers capable of releasing therapeutic cargos at sites of interest in an "on-demand" manner in response to various endogenous (e.g., pH,[3] redox changes,[4] enzymes[5]) or external (e.g., light,[6] magnetic field,[7] ultrasound[8]) stimuli. However, critical issues must be overcome for such stimulus-responsive nanocarriers to be translated into the clinic,[2] including 1) the safety of the materials, since most are made de novo from chemicals or polymers, 2) stimulus sensitivity and response rate, which must be high enough to ensure that sufficient drug is released in the target environment to achieve therapeutic efficacy, and 3) the complexity in the manufacturing process of final nanomedicine with quality control. These performance and manufacturing criteria set a high bar for responsive materials to be considered for use in clinical applications.

Bilirubin is a yellow bile pigment that occurs abundantly in the blood plasma of mammals and acts as a potent endogenous antioxidant that is capable of scavenging various reactive oxygen species (ROS), thereby playing an indispensable role in protecting cells and tissues from oxidative damage.[9] Indeed, numerous epidemiological and experimental studies have demonstrated that bilirubin has intrinsic anti-inflammatory[10] and anticancer[11] activity. In addition to the potential of bilirubin itself as a medicine, we were attracted its unique properties of stimuli responsiveness. Abnormally high levels of serum bilirubin in newborn babies with neonatal jaundice cause brain damage as a result of accumulation of the water-insoluble unconjugated form of bilirubin within it.[12] This condition is treated with blue-light phototherapy in the clinic. What happens during the phototherapy caught our attention. Bilirubin is an extremely hydrophobic and water-insoluble compound because the hydrophilic groups within it, such as carboxylic acids and amide bonds, participate in intramolecular hydrogen bonding interactions (Scheme 1 a). Interestingly, upon irradiation with a proper wavelength of light, bilirubin undergoes photoisomerization (via the breaking of intramolecular hydrogen bonds) and is converted into several photoisomers, all of which have much higher water solubility and thus are easily processed and excreted by the liver and kidneys.[12] On the other hand, ROS exposure causes the oxidation of bilirubin to biliverdin, which also exhibits significantly increased water solubility.[9b,c] This ability to undergo a solubility switch from hydrophobic to hydrophilic in response to two stimuli (intrinsic ROS and external light) suggests that bilirubin could be utilized in a multistimulus-responsive system (Scheme 1). Herein, we provide the first report of bilirubin nanoparticles (BRNPs) as ROS/light-responsive drug-delivery carriers. Our findings demonstrate that BRNPs disassemble in response to both ROS and light, thereby rapidly releasing drugs. Importantly, owing to the intrinsic anticancer and anti-inflammatory effect of bilirubin, BRNPs may be able to function not only as a drug carrier, but also as a therapeutic agent to treat cancers. Very recently, we reported the synthesis, characterization, and therapeutic evaluation of BRNPs in an animal model of inflammatory bowel disease.[13] However, the multistimuli-responsiveness of BRNPs and its potential as a smart drug-delivery carrier have not been investigated in the report.

BRNPs of approximately 95 nm in air-dried form and with a hydrodynamic radius of 105 nm were prepared through the self-assembly of PEGylated bilirubin,[13] a conjugate between bilirubin and polyethylene glycol ($M_w \approx 2{,}000$) via a stable amide bond (Scheme 1 b and Figure S1in the Supporting Information). We next examined whether BRNPs could exhibit stimulus-responsive disruption of the nanostructure. First, the response of BRNPs to a ROS stimulus was tested. The size of the BRNPs upon exposure to ROS generated in aqueous solution by the peroxy radical generator 2,2′-azobis

[*] Dr. Y. Lee, S. Lee, D. Y. Lee, B. Yu, W. Miao, Prof. Dr. S. Jon
KAIST Institute for the BioCentury
Department of Biological Sciences
Korea Advanced Institute of Science and Technology (KAIST)
291 Daehak-ro, Daejeon 34141 (Republic of Korea)
E-mail: syjon@kaist.ac.kr

Supporting information for this article can be found under: http://dx.doi.org/10.1002/anie.201604858.

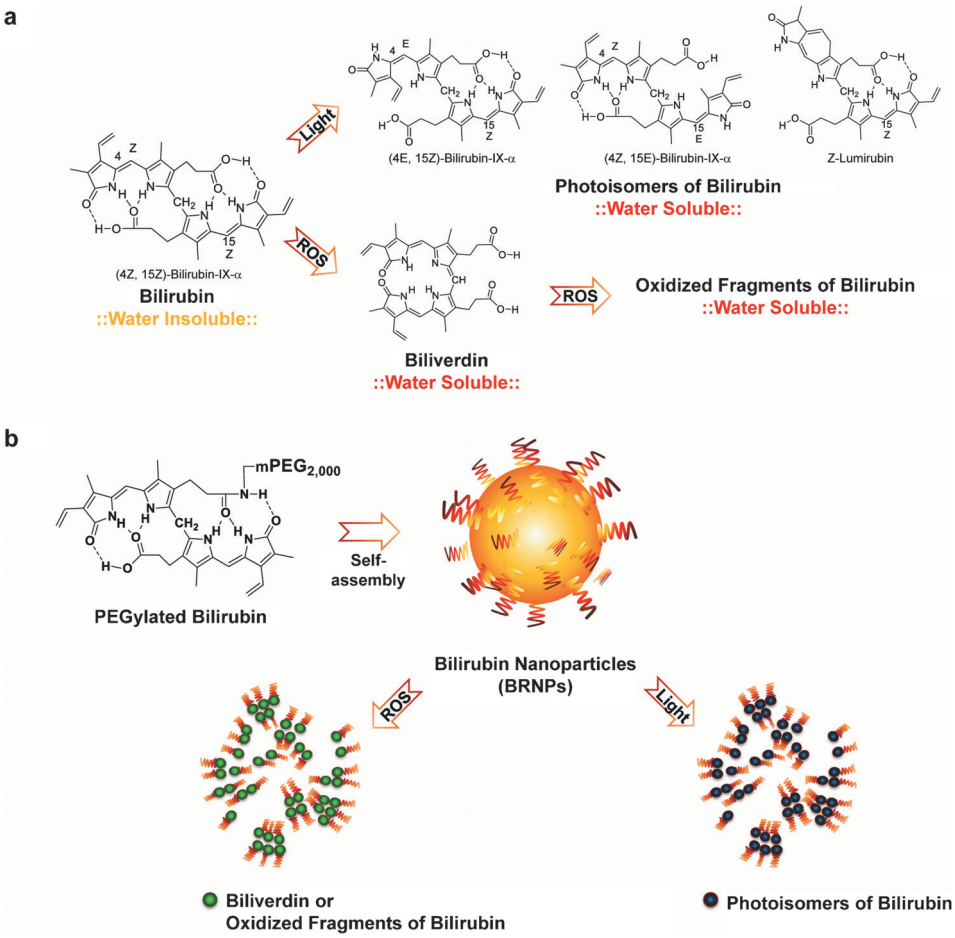

Scheme 1. A) The solubility switch of bilirubin. b) A schematic representation of disruption of the BRNPs in response to light or ROS stimuli.

(2-amidinopropane) dihydrochloride (AAPH) was monitored by dynamic light scattering as a function of time. As shown in Figure 1 a, the BRNPs decreased dramatically in size with a 10 min exposure to the peroxy radicals and were undetectable after a 60 min exposure. An accelerated response of the BRNPs was observed with hypochlorite, which led to complete particle disruption within just 1 min (Figure 1 a). These responses were also easily recognized by the naked eye. As shown in the photographs in Figure 1 a, the aqueous solution of BRNPs, which was initially the yellowish color typical of bilirubin, adopted the greenish blue color characteristic of biliverdin. Eventually, the solution became colorless, which suggests that the bilirubin was first oxidized to biliverdin and then eventually broken down into small oxidized fragments.[9b,c,14] The responsiveness of BRNPs to peroxy radicals was also evaluated by UV/Vis spectrophotometry (Figure S2). Next, we examined the behavior of light-stimulated BRNPs. Exposure of the BRNPs to laser light of either $\lambda = 450$ nm (10 mW cm^{-2}) or $\lambda = 650$ nm (90 mW cm^{-2}) for only 1 min rapidly disrupted the nanoparticles, as shown by the dynamic light scattering measurements (Figure 1 b). This suggests that the bilirubin undergoes a photoisomerization process and is converted into more water-soluble photoisomers,[12] thereby resulting in disassembly of the BRNPs. Taken together, these results indicate that BRNPs undergo ROS- and light-responsive disruption and thus have potential for use as stimulus-responsive drug-delivery carriers.

Next, we examined the suitability of BRNPs for use in cancer therapy. We have shown that the BRNPs are immediately disrupted upon exposure to $\lambda = 450$ nm or 650 nm light as a consequence of a solubility switch from hydrophobic bilirubin to its more hydrophilic photoisomers (see Figure 1 b). The anticancer drug doxorubicin (DOX), was readily loaded into BRNPs through film formation and subsequent rehydration with nearly 100 % efficiency, yielding a maximum loading capacity of approximately 23 wt % (Figure S3). This exceptional loading efficiency and capacity may be attributed to the fact that both bilirubin and DOX have aromatic, planar rings that facilitate packing through π–π interactions and hydrogen bonds.[15] The DOX-loaded BRNPs (DOX@BRNPs) also responded rapidly to irradiation with $\lambda = 650$ nm light (90 mW cm^{-2}, 10 min), which resulted in disruption of the nanoparticles and the simultaneous release of more than 80 % of the drug within 5 min (Figure 2 a). Little drug release was observed in phosphate-buffered saline (PBS, pH 7.4) in the absence of light. Light-triggered drug release by the BRNPs was next evaluated in cancer cells. As shown in Figure 2 b, light stimulation resulted in much greater cellular uptake of DOX than was observed in the absence of irradiation. Likewise, the cytotoxicity of the DOX@BRNPs was much higher in the presence of light than in the absence of light, reaching levels comparable to that of the same amount of free DOX (Figure 2 c). Unlike the drug release profile in a PBS at pH 7.4, it is likely that DOX could be released from the DOX@BRNPs inside cancer cells as a result of intracellular ROS, thereby contributing to the cytotoxicity (Figure 2 c).

We next performed a pharmacokinetic study of the DOX@BRNPs in mice; free DOX was used as a control for comparison. Measurement of DOX concentrations in the bloodstream revealed that the DOX@BRNPs show a much greater area under the curve (AUC), with a much smaller volume of distribution (V_d) than free DOX (Figure 3 a, b); the AUC for the DOX@BRNPs was around 56-fold greater than

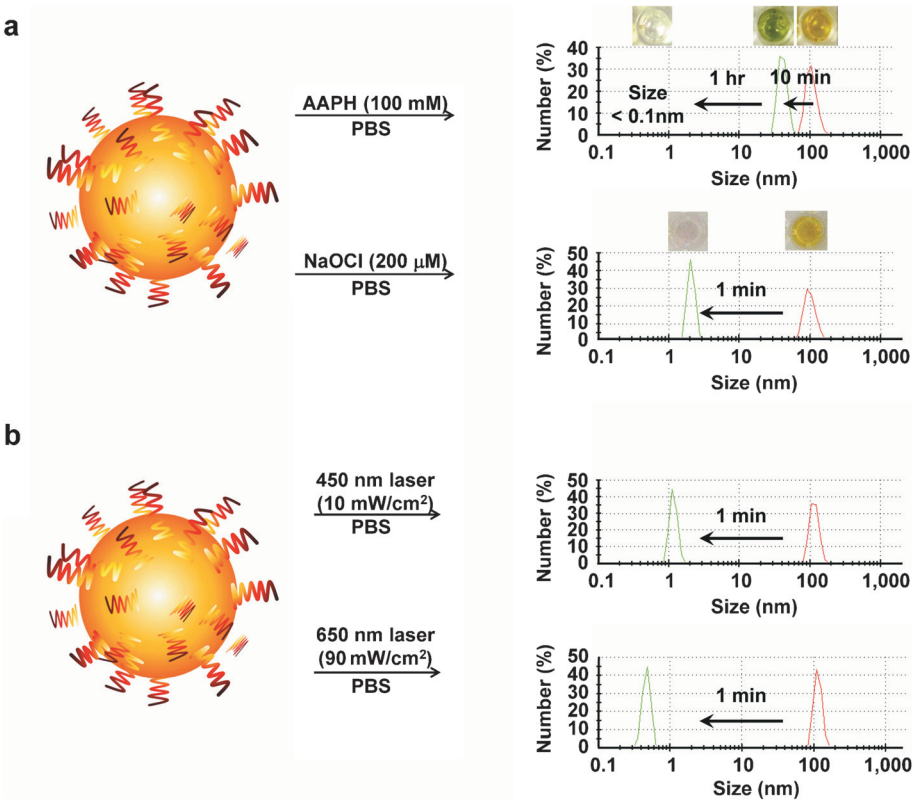

Figure 1. Multistimulus-responsive BRNPs formed from PEG-BR. Changes in the size of the BRNPs (in PBS) induced by ROS (a) or light (b) stimuli were determined by dynamic light scattering. The BRNPs were exposed to the peroxy radical generator AAPH (100 mM) or sodium hypochloride (200 μM), or were irradiated with a $\lambda = 450$ nm (10 mW cm^{-2}) or 650 nm (90 mW cm^{-2}) laser for 1 min.

that for free DOX. Pharmacokinetic data obtained through direct measurement of BRNP concentrations in the bloodstream followed a similar trend (Figure S4), thus suggesting that most of the DOX@BRNPs circulate in the blood without leaking the drug.

Encouraged by the in vitro cytotoxicity and in vivo pharmacokinetic data, we next assessed the anticancer efficacy of the DOX@BRNPs, with and without laser irradiation, in xenografted mice bearing human lung adenocarcinoma cell (A549) tumors. After the tumors reached a size of approximately 90 mm^3, the mice were intravenously administered with the DOX@BRNPs (2 mg kg^{-1}), free DOX (2 mg kg^{-1}), or PBS (control) every 3 days for a total of five injections, and tumor growth was assessed on day 19. As shown in Figure 3c, tumor growth in the mice treated with free DOX was inhibited by 27.8% relative to that observed in the control group (PBS treatment), whereas tumor growth in the DOX@BRNPs group was inhibited by 55.0%. Notably, laser irradiation ($\lambda = 650$ nm, 200 mW cm^{-2}, 5 min) further significantly enhanced the efficacy of the DOX@BRNPs, leading to tumor growth inhibition of up to 71.9% (Figure 3c). Interestingly, treatment with the BRNPs alone inhibited tumor growth by 38.1%, thus indicating that the BRNPs, like free bilirubin, also retain intrinsic anticancer efficacy.[11] It has been reported that some antioxidant compounds and polymers exhibit anticancer activity by inhibiting angiogenesis in the tumor tissue environment.[11c,16] To determine whether the BRNPs affect angiogenesis, we performed tube-formation assays using human umbilical vein endothelial cells (HUVECs).[11c,17] These assays showed that the BRNPs profoundly inhibit tube formation, thus suggesting that they may exert their anticancer activity by inhibiting angiogenesis (Figure S5), although the precise mechanism remains to be elucidated. In contrast to free DOX, which was overtly toxic, BRNP treatment was not associated with appreciably toxicity, as measured by body weight loss (Figure 3d). Taken together, our results indicate that the DOX@BRNPs prolong the life of the parenteral drug in the circulation and release the drug in response to an external light stimulus at the tumor site, thereby exerting potent antitumor efficacy. In addition, the anticancer effect of the BRNPs themselves may further enhance the therapeutic efficacy of the DOX@BRNPs.

In conclusion, we have developed a multistimulus-responsive nanomedicine that enables controlled drug delivery and release, while simultaneously exerting potent therapeutic activity in its own right against cancer. These nanocarriers, formed from PEGylated bilirubin, exhibited rapid and highly sensitive stimulus-responsive disruption upon exposure to either ROS or light with wavelengths of $\lambda = 450$ or 650 nm. The BRNPs were capable of loading anticancer drugs with high efficiency and capacity, prolonged the residence time of the drug in the circulation, exerted antiangiogenic effects, and significantly enhanced the efficiency of tumor-growth inhibition, especially in combination with exposure to external $\lambda = 650$ nm light. Moreover, the BRNPs are composed entirely of PEGylated bilirubin, which can be synthesized on a large scale as a pure chemical entity after conventional column chromatography. Likewise, the BRNP preparation process is quite simple and is applicable to large-scale production, thus suggesting that it should be possible to translate our BRNPs into the clinic. Altogether, these BRNPs show great potential as a combined drug-delivery carrier and medicine to treat a variety of cancers.

Acknowledgements

This work was supported by a Global Research Laboratory grant (2015045887) and the KAIST Future Systems Health-

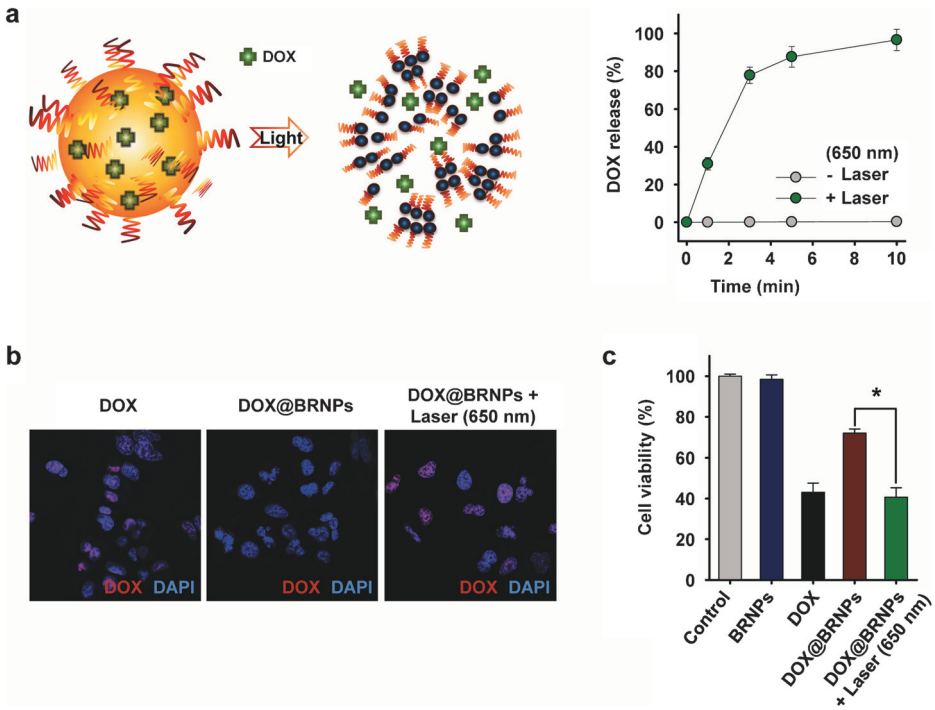

Figure 2. DOX@BRNPs as light-responsive nanoparticles that can be used in antitumor phototherapy. a) DOX release from the DOX@BRNPs in the absence and presence of $\lambda = 650$ nm laser irradiation (90 mW cm^{-2}, 10 min). Data are presented as the mean ± SD ($n = 5$). b) A confocal fluorescence image of A549 cells treated with culture medium, free DOX (10 μM), the BRNPs (10 μM), the DOX@BRNPs (10 μM DOX; 10 μM BRNPs), or the DOX@BRNPs for 4 h with $\lambda = 650$ nm laser irradiation (90 mW cm^{-2}, 5 min). DOX (red) and nuclei (blue) were visualized. c) Cell viability of A549 cells incubated with culture medium (control), DOX (10 μM), the BRNPs (10 μM), the DOX@BRNPs (10 μM DOX; 10 μM BRNPs), or the DOX@BRNPs for 4 h with $\lambda = 650$ nm laser irradiation (90 mW cm^{-2}, 5 min). Data are presented as the mean ± SEM. ($n = 6$; *$p < 0.001$, one-way ANOVA).

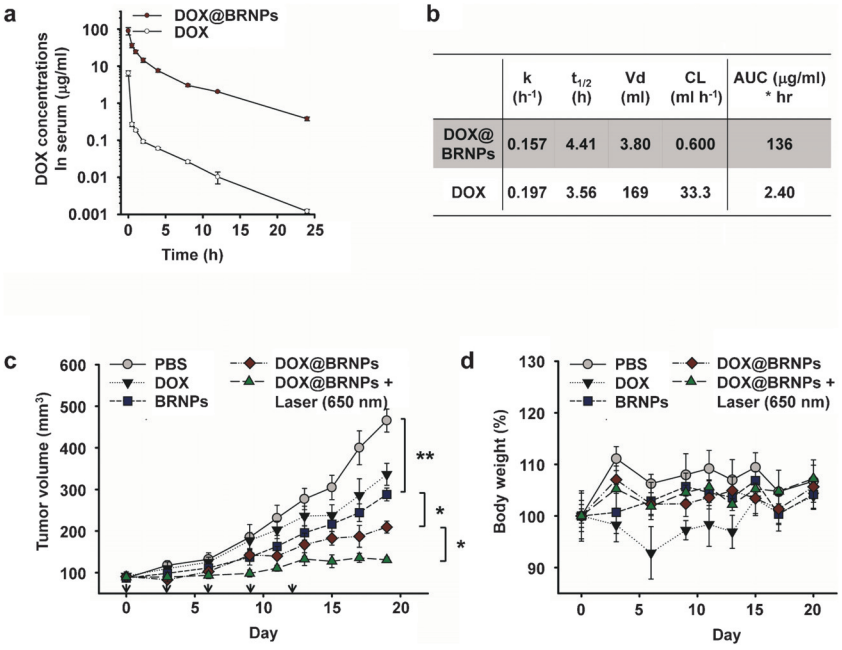

	k (h^{-1})	$t_{1/2}$ (h)	Vd (ml)	CL (ml h^{-1})	AUC (μg/ml) * hr
DOX@ BRNPs	0.157	4.41	3.80	0.600	136
DOX	0.197	3.56	169	33.3	2.40

Figure 3. The DOX@BRNPs combined with laser irradiation show improved anticancer activity compared to the drug-loaded nanoparticles alone. Serum concentration (a) and pharmacokinetic profile (b) of DOX from mice treated with free DOX (4 mg kg^{-1}), or the DOX@BRNPs (40 mg kg^{-1}; equivalent to 4 mg DOX k^{-}) through intravenous injection. Data are presented as the mean ± SD ($n = 5$). c, d) Mice bearing tumors (size > 90 mm^2) were intravenously administered with PBS, free DOX (2 mg kg^{-1}), the BRNPs (20 mg kg^{-1}), the DOX@BRNPs (20 mg kg^{-1}; equivalent to 2 mg DOX kg^{-1}), or the DOX@BRNPs with a laser irradiation ($\lambda = 650$ nm, 90 mW cm^{-2}) for 5 min. Tumor volume (c) and body weight (d) were measured on predetermined days. Data are presented as the mean ± SEM. ($n = 5$; *P < 0.05, **$p < 0.001$, one-way ANOVA).

care Project through the National Research Foundation of Korea (NRF), funded by the Ministry of Science, ICT & Future Planning.

Keywords: anticancer therapy · bilirubin · drug delivery · nanomedicine · nanoparticles

How to cite: *Angew. Chem. Int. Ed.* **2016**, *55*, 10676–10680
Angew. Chem. **2016**, *128*, 10834–10838

[1] M. B. Yatvin, J. N. Weinstein, W. H. Dennis, R. Blumenthal, *Science* **1978**, *202*, 1290–1293.
[2] a) S. Mura, J. Nicolas, P. Couvreur, *Nat. Mater.* **2013**, *12*, 991–1003; b) V. P. Torchilin, *Nat. Rev. Drug Discovery* **2014**, *13*, 813–827.
[3] a) M. F. Chung, H. Y. Liu, K. J. Lin, W. T. Chia, H. W. Sung, *Angew. Chem. Int. Ed.* **2015**, *54*, 9890–9893; *Angew. Chem.* **2015**, *127*, 10028–10031; b) S. Nowag, R. Haag, *Angew. Chem. Int. Ed.* **2014**, *53*, 49–51; *Angew. Chem.* **2014**, *126*, 51–53.
[4] a) M. Wang, S. Sun, C. I. Neufeld, B. Perez-Ramirez, Q. Xu, *Angew. Chem. Int. Ed.* **2014**, *53*, 13444–13448; *Angew. Chem.* **2014**, *126*, 13662–13666; b) M. S. Shim, Y. Xia, *Angew. Chem. Int. Ed.* **2013**, *52*, 6926–6929; *Angew. Chem.* **2013**, *125*, 7064–7067.
[5] Z. Liu, M. Xiong, J. Gong, Y. Zhang, N. Bai, Y. Luo, L. Li, Y. Wei, Y. Liu, X. Tan, R. Xiang, *Nat. Commun.* **2014**, *5*, 4280.
[6] a) Z. Xiao, C. Ji, J. Shi, E. M. Pridgen, J. Frieder, J. Wu, O. C. Farokhzad, *Angew. Chem. Int. Ed.* **2012**, *51*, 11853–11857; *Angew. Chem.* **2012**, *124*, 12023–12027; b) N. C. Fan, F. Y. Cheng, J. A. Ho, C. S. Yeh, *Angew. Chem. Int. Ed.* **2012**, *51*, 8806–8810; *Angew. Chem.* **2012**, *124*, 8936–8940.
[7] M. H. Cho, E. J. Lee, M. Son, J. H. Lee, D. Yoo, J. W. Kim, S. W. Park, J. S. Shin, J. Cheon, *Nat. Mater.* **2012**, *11*, 1038–1043.
[8] J. Y. Lee, D. Carugo, C. Crake, J. Owen, M. de Saint Victor, A. Seth, C. Coussios, E. Stride, *Adv. Mater.* **2015**, *27*, 5484–5492.
[9] a) R. Stocker, Y. Yamamoto, A. F. McDonagh, A. N. Glazer, B. N. Ames, *Science* **1987**, *235*, 1043–1046; b) D. E. Baranano, M. Rao, C. D. Ferris, S. H. Snyder, *Proc. Natl. Acad. Sci. USA* **2002**, *99*, 16093–16098; c) T. W. Sedlak, M. Saleh, D. S. Higginson, B. D. Paul, K. R. Juluri, S. H. Snyder, *Proc. Natl. Acad. Sci. USA* **2009**, *106*, 5171–5176.
[10] a) S. J. Kang, D. Kim, H. E. Park, G. E. Chung, S. H. Choi, S. Y. Choi, W. Lee, J. S. Kim, S. H. Cho, *Atherosclerosis* **2013**, *230*, 242–248; b) S. Jangi, L. Otterbein, S. Robson, *Int. J. Biochem. Cell Biol.* **2013**, *45*, 2843–2851; c) R. Öllinger, H. Wang, K. Yamashita, B. Wegiel, M. Thomas, R. Margreiter, F. H. Bach, *Antioxid. Redox Signaling* **2007**, *9*, 2175–2185.
[11] a) L. J. Horsfall, G. Rait, K. Walters, D. M. Swallow, S. P. Pereira, I. Nazareth, I. Petersen, *JAMA J. Am. Med. Assoc.* **2011**, *305*, 691–697; b) S. D. Zucker, P. S. Horn, K. E. Sherman, *Hepatology* **2004**, *40*, 827–835; c) J. Zheng, D. A. Nagda, S. A. Lajud, S. Kumar, A. Mouchli, O. Bezpalko, B. W. O'Malley, Jr., D. Li, *Br. J. Cancer* **2014**, *110*, 2116–2122; d) R. Ollinger, P. Kogler, J. Troppmair, M. Hermann, M. Wurm, A. Drasche, I. Konigsrainer, A. Amberger, H. Weiss, D. Ofner, F. H. Bach, R. Margreiter, *Cell Cycle* **2007**, *6*, 3078–3085; e) P. Rao, R. Suzuki, S. Mizobuchi, T. Yamaguchi, S. Sasaguri, *Biochem. Biophys. Res. Commun.* **2006**, *342*, 1279–1283.
[12] M. J. Maisels, A. F. McDonagh, *N. Engl. J. Med.* **2008**, *358*, 920–928.
[13] Y. Lee, H. Kim, S. Kang, J. Lee, J. Park, S. Jon, *Angew. Chem. Int. Ed.* **2016**, *55*, 7460–7463; *Angew. Chem.* **2016**, *128*, 7586–7589.
[14] G. J. Maghzal, M. C. Leck, E. Collinson, C. Li, R. Stocker, *J. Biol. Chem.* **2009**, *284*, 29251–29259.
[15] X. Deng, X. Xu, Y. Lai, B. He, Z. Gu, *J. Biomed. Nanotechnol.* **2013**, *9*, 1336–1344.
[16] a) M. Moriyama, S. Metzger, A. J. van der Vlies, H. Uyama, M. Ehrbar, U. Hasegawa, *Adv. Healthcare Mater.* **2015**, *4*, 569–575; b) S. Giri, A. Karakoti, R. P. Graham, J. L. Maguire, C. M. Reilly, S. Seal, R. Rattan, V. Shridhar, *PloS one* **2013**, *8*, e54578.
[17] B. D. Wilson, M. Ii, K. W. Park, A. Suli, L. K. Sorensen, F. Larrieu-Lahargue, L. D. Urness, W. Suh, J. Asai, G. A. Kock, T. Thorne, M. Silver, K. R. Thomas, C. B. Chien, D. W. Losordo, D. Y. Li, *Science* **2006**, *313*, 640–644.

Received: May 18, 2016
Revised: June 20, 2016
Published online: August 2, 2016

